Weathering Processes in the Icacos and Mameyes Watersheds in Eastern Puerto Rico

By Heather L. Buss and Arthur F. White

Chapter I of
Water Quality and Landscape Processes of Four Watersheds in Eastern Puerto Rico
Edited by Sheila F. Murphy and Robert F. Stallard

Professional Paper 1789–I

U.S. Department of the Interior
U.S. Geological Survey

Contents

Figures

Abbreviations Used in This Report

≈	nearly equal to
^{30}Si	ratio of stable isotopes of silicon, $^{30}Si/^{28}Si$, relative to a standard
Å	angstrom
μmol mol^{-1}	micromoles per mole
cm	centimeter
km^2	square kilometer
m	meter
Ma	million years old
m $m.y.^{-1}$	meters per million years
mol m^{-2} s^{-1}	moles per square meter per second
ICP–OES	inductively coupled plasma–atomic emission spectroscopy
WEBB	Water, Energy, and Biogeochemical Budgets
XRD	X-ray diffraction

Conversion Factors

Multiply	By	To obtain
	Length	
centimeter (cm)	0.3937	inch (in.)
meter (m)	3.281	foot (ft)
	Area	
square kilometer (km^2)	0.3861	square mile (mi^2)
	Weathering rate	
meters per million years (m $m.y.^{-1}$)	3.281	feet per million years (ft $m.y.^{-1}$)

Weathering Processes in the Icacos and Mameyes Watersheds in Eastern Puerto Rico

By Heather L. Buss and Arthur F. White

Abstract

Streams draining watersheds of the two dominant lithologies (quartz diorite and volcaniclastic rock) in the Luquillo Experimental Forest of eastern Puerto Rico have very high fluxes of bedrock weathering products. The Río Blanco quartz diorite in the Icacos watershed and the Fajardo volcaniclastic rocks in the Mameyes watershed have some of the fastest documented rates of chemical weathering of siliceous rocks in the world. Rapid weathering produces thick, highly leached saprolites in both watersheds that lie just below the soil and largely isolate subsurface biogeochemical and hydrologic processes from those in the soil. The quartz diorite bedrock in the Icacos watershed weathers spheroidally, leaving large, relatively unweathered corestones that are enveloped by slightly weathered rock layers called rindlets. The rindlets wrap around the corestones like an onionskin.

Within the corestones, biotite oxidation is thought to induce the spheroidal fracturing that leads to development of rindlets; plagioclase in the rindlets dissolves, creating additional pore spaces. Near the rindlet-saprolite interface, the remaining plagioclase dissolves, hornblende dissolves to completion, and precipitation of kaolinite, gibbsite, and goethite becomes pervasive. In the saprolite, biotite weathers to kaolinite and quartz begins to dissolve. In the soil layer, both quartz and kaolinite dissolve. The volcaniclastic bedrock of the Mameyes watershed weathers even faster than the quartz diorite bedrock of the Icacos watershed, leaving thicker saprolites that are devoid of all primary minerals except quartz. The quartz content of volcaniclastic bedrock may help to control watershed geomorphology; high-quartz rocks form thick saprolites that blanket ridges.

Hydrologic flow paths within the weathering profiles vary with total fluid flux, and they influence the chemistry of streams. Under low-flow conditions, the Río Icacos and its tributaries are fed by rainfall and by groundwater from the fracture zones; during storm events, intense rainfall rapidly raises stream levels and water is flushed through the soil as shallow flow. As a result, weathering constituents that shed into streamwaters are dominated by rindlet-zone weathering processes during base flow and by soil weathering processes during stormflow. The upper reaches of the Mameyes watershed are characterized by regolith more than 35 meters thick in places that contains highly fractured rock embedded in its matrix. Weathering contributions to stream chemistry at base flow are predicted to be more spatially variable in the Mameyes watershed than in the Icacos watershed owing to the more complex subsurface weathering profile of the volcaniclastic bedrocks of the Mameyes watershed.

Introduction

Biogeochemical and physical weathering processes in tropical watersheds produce most of the solutes and sediments discharged to the oceans. These watersheds contribute 50 percent of the water, 38 percent of the dissolved ions, and 65 percent of the dissolved silica in the oceans, despite covering only about 25 percent of the terrestrial surface (Stallard and Edmond, 1983; Meybeck, 1987). Thus, relative to their area, tropical systems are disproportionately important in terms of weathering, erosion, and global CO_2 cycles. In addition to influencing stream and ocean chemistry and sediment loads, weathering processes exert control over chemical transport through soils and regolith (such as saprolite), soil and saprolite formation rates, mineral nutrient availability, and microbial growth rates. Weathering processes are complex phenomena comprising coupled chemical, physical, and microbial processes, driven by water and oxygen fluxes. These coupled processes also control the shape, position, stability, and rate of retreat of the bedrock weathering interface, which in turn affect topography and erosion.

To date (2012), the majority of research into weathering processes in the four U.S. Geological Survey Water, Energy, and Biogeochemical Budgets program (WEBB) watersheds in eastern Puerto Rico has focused on the Icacos watershed. This watershed is an ideal site for studying tropical weathering processes, because it is relatively pristine, small (3.3 square kilometers (km^2)), and lithologically homogeneous (99 percent Río Blanco quartz diorite; Murphy and others, 2012). Thick saprolite profiles on ridge tops allow analysis of deep weathering and the cycling of chemical elements—processes that are not directly coupled with the surficial environment. The homogeneity of the quartz diorite (relative to the volcaniclastic units that dominate the Mameyes watershed) also considerably simplifies interpretation of the weathering profiles. Currently, a subwatershed of the

Mameyes watershed, Bisley 1 (fig. 1), is being investigated and compared with the Icacos watershed in order to better understand the influence of lithology on weathering processes, weathering fluxes, and mineral nutrient availability.

Weathering processes within the Bisley 1 watershed are spatially more variable than in the Icacos watershed owing to the more varied lithology of the parent rock. The Bisley 1 watershed is underlain by the Fajardo Formation, a marine-bedded volcaniclastic bedrock that is mapped as having several units: an upper thin-bedded tuffaceous siltstone and sandstone, an upper thick-bedded tuff, a lower thin-bedded tuffaceous sandstone and siltstone, a lower thick-bedded tuff, and an undivided unit (Briggs and Aguilar-Cortés, 1980). Bed thicknesses differ, and coarse tuff, breccias, and cherty or calcareous siltstone beds are found in some units. Although the few bedrock exposures in the Bisley watershed appear homogeneous, the watershed is underlain by the upper thick-bedded tuff unit, which includes some breccias, lithic andesitic clasts, calcareous siltstone, and some pumice and red scoria. Spheroidally weathered, marine-bedded, volcaniclastic sandstones are occasionally exposed by landslides. Weathered, quartz-rich clasts, which may be relict quartz veins, are found in the Bisley regolith.

In contrast to the high quartz content of the Río Blanco quartz diorite (≈20–30 percent by weight; White and others, 1998; Turner and others, 2003; Buss and others, 2008), which creates a weathering-resistant matrix that supports isovolumetric weathering to form saprolite, the bluish-gray tuffaceous rock commonly found in the Bisley streambeds contains very little quartz (≈7 percent, as analyzed by X-ray diffraction (XRD) and quantified using the program RockJock as described by Eberl, 2003). Without a quartz matrix to support the volume during chemical weathering, these volcaniclastic rocks likely dissolve completely or collapse in volume during weathering. However, quartz-rich saprolites (as much as 65 percent) greater than 35 meters (m) deep are found in the Bisley watershed, indicating formation from a parent rock with a higher quartz content than the rocks commonly encountered in the Bisley watershed today. Similar rocks, but with higher quartz content (≈22–27 percent) may be exposed after relatively deep landslides in the Bisley 1 watershed and within a few kilometers to the east. These rocks may have been hydrothermally altered by infiltrating Si-rich fluids during intrusion of the Río Blanco stock. Thus, saprolite-mantled ridges in the Bisley watershed likely formed from these relatively quartz-rich rocks.

Both the quartz-rich and quartz-poor volcaniclastic rocks in the Bisley watershed contain similar amounts of chlorite (20–25 percent) and pyroxene (5–10 percent), but they diverge in feldspar content: about 35 and 50 percent, respectively. The Bisley saprolite contains ≈15–65 percent microcrystalline quartz into which are embedded sparse, small, weathered, quartz-rich clasts (as much as ≈80 percent quartz) that may represent relict quartz veins. Typically, quartz content by weight is higher in weathered materials, such as saprolite, relative to the parent rock. When other minerals weather and elements such as Ca, Na, Mg, and K are lost from the system, quartz makes up a larger proportion of the remaining mass than it did originally. Similarly, elements that are relatively immobile during chemical weathering, such as Ti and Zr, are also more abundant in saprolite relative to parent rock in both the Bisley watershed (bulk chemistry measured by inductively coupled plasma–atomic emission spectroscopy (ICP–OES) after lithium metaborate fusion) and Icacos watershed (White and others, 1998; Buss and others, 2005, 2008).

The Fajardo Formation, which underlies the Bisley watershed, is older than the granitic intrusion underlying the Icacos watershed, ≈100 million years old (Ma) as compared with 47 Ma, respectively (Jolly and others, 1998; Smith and others, 1998). Regolith in the Bisley 1 watershed is also thicker than in the Icacos watershed: about 10–20 m and 5–9 m on ridge tops in the Bisley and Icacos watersheds, respectively (White and others, 1998; Schellekens and others, 2004; Buss and others, 2005). Borehole drilling on a road in the Bisley 1 watershed recovered regolith cores more than 35 m deep, within which were embedded highly fractured rock in varying stages of weathering. These cores may contain a combination of transported material (such as from old landslides) and saprolite (which is formed in place, by definition). A 29-m-deep borehole on a road in the Icacos watershed passed through 5 m of saprolite, followed by a fractured-bedrock zone less than 1 m thick, and finally through 23 m of solid, unfractured, quartz diorite bedrock. A saprolite-production rate (or bedrock-weathering rate) of 211 meters per million years (m m.y.$^{-1}$) has been estimated for a Bisley ridgetop (Dosetto and others, 2011), which is considerably faster than the 43–58 m m.y.$^{-1}$ rate estimated for the Icacos watershed (Brown and others, 1995; White and others, 1998; Riebe and others, 2003, 2004). The bedrock weathering rates of both watersheds are also high relative to weathering rates of siliceous bedrock (such as basalts, andesites, granitoids, and schists) in watersheds around the world (White and others, 1998; Freyssinet and Farah, 2000; Navarre-Sitchler and Brantley, 2007; Dosseto and others, 2011).

The Bisley saprolite is about 60–80 weight percent clay (primarily microcrystalline, disordered kaolinite) and is completely devoid of primary minerals except quartz, indicating an advanced stage of weathering (mineralogy analyzed by XRD). The kaolinite contains impurities of Mg, Fe, and K that are released as the kaolinite itself dissolves with time. The Icacos saprolite contains primary biotite, which releases appreciable Mg, K, and Fe during transformation to kaolinite throughout the saprolite (Murphy and others, 1998).

The remainder of this chapter discusses weathering processes in the Icacos watershed (fig.1), which has been studied in much greater detail than the Mameyes watershed. The Río Blanco quartz diorite weathers in place along joint planes, forming rounded bedrock corestones (as much as about 2 m diameter), which then weather spheroidally (fig. 2). Onionskin-like layers (rindlets) form on the corestones during spheroidal weathering; continued weathering of the corestones produces a thick (about 2–8 m) saprolite overlain by

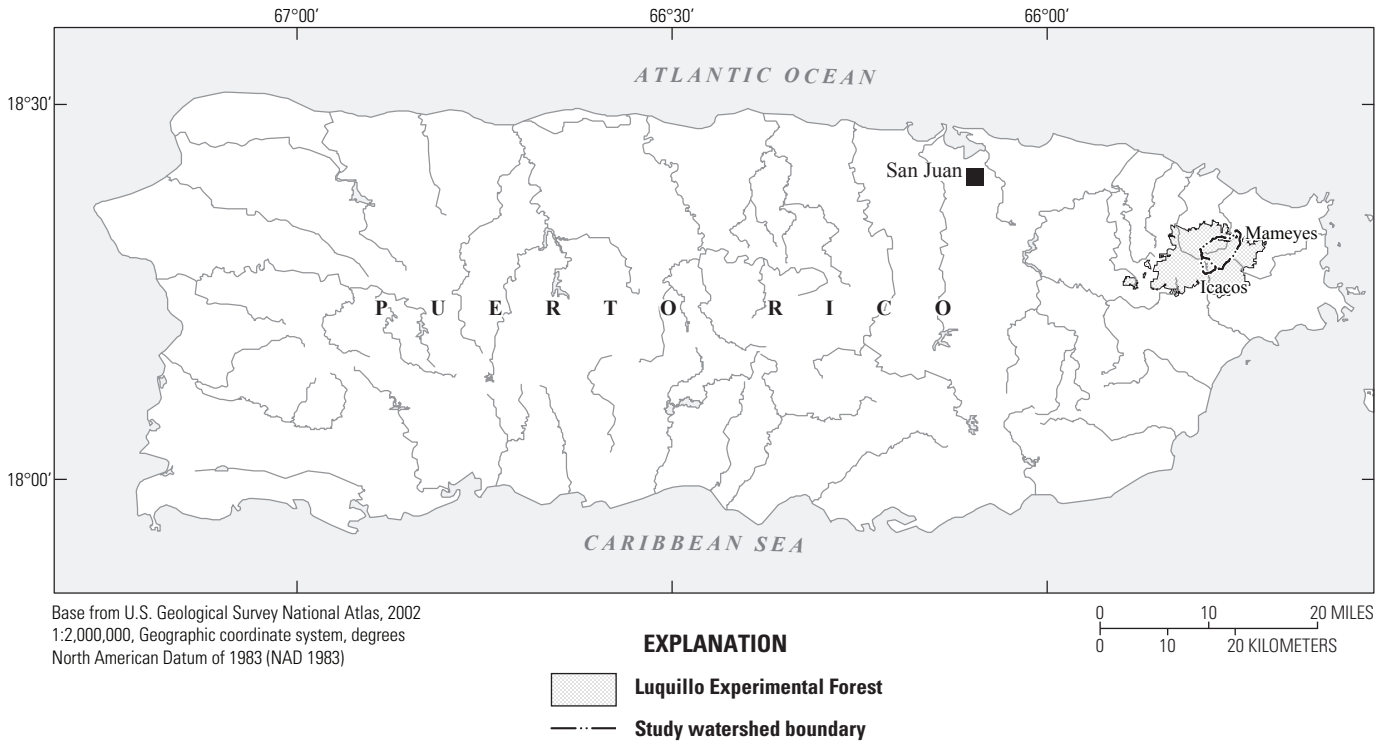

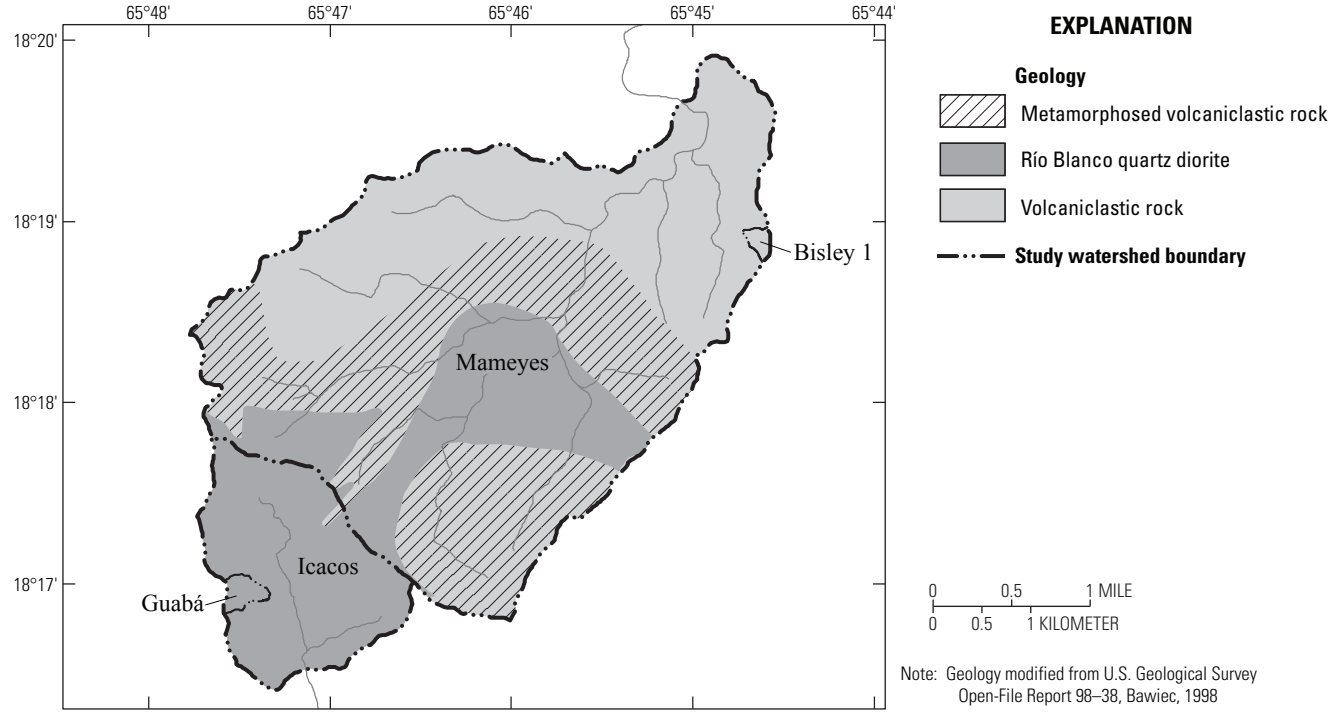

Figure 1. Location and geology of Icacos and Mameyes watersheds. (Geology adapted from Bawiec (1998); metamorphic contact from Seiders (1971) and Briggs and Aguilar-Cortés (1980), with digital interpretation by F.N. Scatena and Miguel Leon, University of Pennsylvania Luquillo Critical Zone Observatory; Bisley 1 watershed boundary courtesy Miguel Leon, University of Pennsylvania; Guabá watershed boundary courtesy Sheila Murphy, U.S. Geological Survey.)

Figure 2. Sampled roadcut 600 meters southeast of the mouth of the Icacos watershed showing a 2-meter diameter corestone of Río Blanco quartz diorite that is weathering spheroidally. A 49-centimeter-thick zone of partially weathered rock layers called rindlets surrounds the corestone. The string grid (at an angle to the camera) partitions the outcrop into 1-square-meter blocks.

thin (about 0.5–1 m) soils. The resulting weathering profile is characterized by multiple interfaces that define distinct zones in which weathering processes differ and, in some cases, operate independently of the processes operating within the other zones. Here we will discuss weathering processes in individual zones from the fresh bedrock upward to the surface soil.

Weathering Processes at the Bedrock Interface

Weathering of fresh, intact bedrock is the initial step in the soil-forming process and is the primary contributor of chemical solutes to the hydrosphere—groundwater, streams, precipitation, and oceans. Interfaces where intact bedrock weathers to disaggregated material, such as saprolite, are controlled by coupled chemical, physical, and microbial processes driven by the flux of reactants to the fresh rock. The rate at which the bedrock weathers determines the rate at which the interface moves downward, the rate of formation of the saprolite, the flux of mineral nutrients to the biosphere, and the flux of solutes to the hydrosphere.

A spheroidally weathering interface, such as in the Río Blanco quartz diorite, provides a model environment for studying the coupling of physical and chemical processes involved in rock weathering and saprolite formation. Spheroidal weathering is a well-known, but poorly understood, form of exfoliation that has been linked to chemical weathering (for example, Farmin, 1937; Ollier, 1971; Fletcher and others, 2006; Buss and others, 2008). Spheroidal weathering begins when bedrock joint planes are exposed to weathering, which rounds off corners in place to form boulders called corestones. Corestones then fracture parallel to and just below their surface, forming concentric layers called rindlets (Bisdom, 1967; Ollier, 1971; Fritz and Ragland, 1980; Turner and others, 2003; Buss and others, 2005, 2008). A complete set of rindlets (from corestone to saprolite) comprise a rindlet zone (fig. 3).

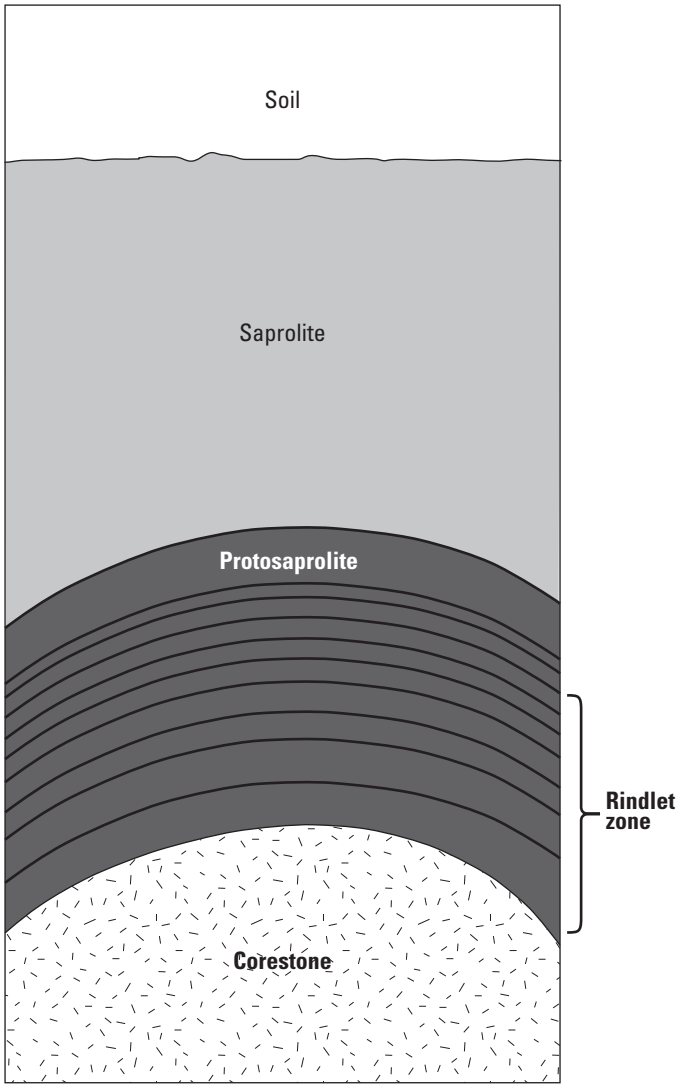

Figure 3. Generalized view of the weathering profile in the Icacos watershed. Quartz diorite bedrock corestones weather spheroidally, producing a zone of concentric layers called rindlets. Rindlets transform into saprolite in a zone called protosaprolite or saprock, where weathering processes differ from those in either the rindlet zone or saprolite (Buss and others, 2008).

Rindlets are slightly weathered, but most are still relatively hard. The hand-friable outer rindlets (at the saprolite interface) are sometimes referred to as *saprock,* a material intermediate between saprolite and bedrock. Where rindlet zones are exposed by erosion (which is dominated by landslides; Larsen and Torres-Sánchez, 1998), they tend to slough off, leaving bare corestones. Corestone-rindlet complexes that remain in place at depth eventually weather to saprolite.

Expansion of a mineral during chemical weathering has been identified as a possible cause of spheroidal fracturing (for example, Larsen, 1948; Simpson, 1964; Eggler and others, 1969; Isherwood and Street, 1976; Begle, 1978; Chatterjee and Raymahashay, 1998; Fletcher and others, 2006; Buss and others, 2008). Although isovolumetric weathering is required to produce the overlying saprolite, Fletcher and others (2006) demonstrated quantitatively that only a very small net volume change is required to generate sufficient elastic strain energy to produce spheroidal fracturing as observed in the Río Blanco quartz diorite.

The rindlet zone in the Río Blanco quartz diorite is composed of a sequence of rindlets each about 2.5 centimeters (cm) thick, which are slightly weathered relative to the parent corestones (fig. 4). Within the rindlet zone, the transformation from bedrock to saprolite is accomplished. This transformation includes development of pore space, essentially complete loss (≈99 percent) of the primary minerals plagioclase, hornblende, chlorite, and apatite; oxidation of biotite; and formation of the secondary minerals kaolinite, gibbsite, and goethite (Buss and others, 2008, 2010). These weathering processes occur at different points within the rindlet zone but are interrelated. The transformation of bedrock to saprolite begins within the corestones. Aqueous oxygen contained in pore waters diffuses into the unweathered corestone and oxidizes Fe(II) in the biotite (Buss and others, 2008), which then expands in the d(001) direction from 10.0 angstroms (Å) to 10.5 Å (Dong and others, 1998; Murphy and others, 1998). This modest expansion builds up elastic strain energy within the rock (Buss and others, 2008). When the elastic-strain-energy density reaches fracture surface energy, fracturing occurs, creating a rindlet (Fletcher and others, 2006). The oxidation of Fe(II) in biotite is initiated when dissolved oxygen diffuses into the corestones; thus the weathering rate depends on the concentration of oxygen in pore waters. This concentration is expected to decrease with increasing saprolite thickness, creating a positive feedback between erosion and weathering rates that may maintain profiles at steady state throughout geologic time (Fletcher and others, 2006).

A weathering front is a boundary layer, or zone, that separates weathered material from fresh rock. It is often defined in terms of a weathering reaction (for example, dissolution of a given mineral) such that the weathering front encompasses the entire zone where the weathering reaction occurs. For a mineral weathering reaction, the mineral becomes progressively more altered (or changes in abundance) within the weathering front. Turner and others (2003) conceptualized the spheroidal weathering system in the Río Blanco quartz diorite as consisting of many parallel weathering fronts that move inward toward each of the rindlet centers from their edges as well as inward towards the centers of the corestones. However, in detailed analyses of a complete rindlet sequence, Buss and others (2008) did not detect a trend in chemical weathering intensity within individual rindlets and proposed an alternative model. In this model, the entire rindlet zone and corestone is a single weathering front controlled by only two interfaces: the bedrock-rindlet interface and the rindlet-saprolite interface, which are coupled by the pore-space-forming processes of mineral dissolution and fracturing.

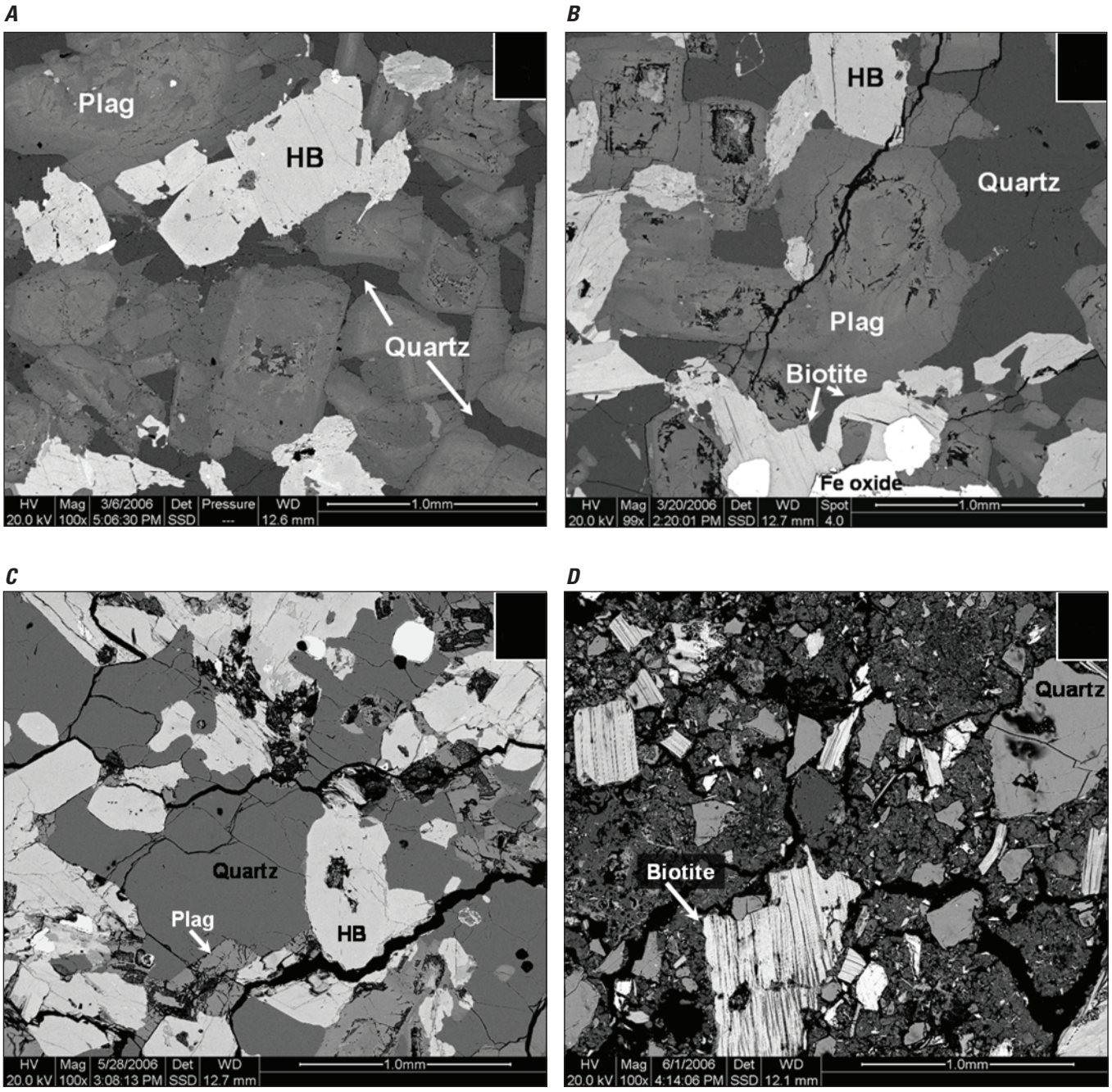

Figure 4. Backscattered electron images of thin sections taken from a corestone-rindlet complex exposed at a roadcut 600 meters southeast of the mouth of the Icacos watershed. *A*, Corestones are relatively unweathered and unfractured and are dominated by large zoned plagioclase crystals. *B*, A typical rindlet sampled from about 20 centimeters above the corestone (the entire rindlet sequence was 49 centimeters thick) contains microcracks, unaltered hornblende (HB), and pore space within plagioclase (Plag) crystals where calcic cores are weathering before sodic edges. *C*, Within the protosaprolite zone, a rindlet sampled from about 2 centimeters below the visible rindlet-saprolite interface contains unaltered quartz, highly weathered plagioclase (Plag) with gibbsite and kaolinite within the pore spaces, and slightly weathered hornblende (HB). *D*, Also within the protosaprolite zone, a sample taken from about 0.5 centimeter above the visible rindlet-saprolite interface contains quartz and visibly altered biotite; hornblende and plagioclase crystals are no longer visible. Large areas are filled with gibbsite and kaolinite (after Buss, 2006; Buss and others, 2008).

In a one-dimensional, steady-state profile, the loss of a mobile element or dissolving mineral can be modeled as a linear decrease with decreasing depth from the parent rock composition to some weathered composition. This linear decrease, or weathering gradient, is composed of two vectors: the weathering velocity (which equals rate of advance of the weathering front in a solid-state profile or the fluid flux in an aqueous profile) and the rate of loss of the individual mineral or element that defines the gradient (White, 2002). Solid-state gradients in Na, Fe(II), and P within a rindlet zone were used to calculate weathering rates for plagioclase dissolution (Na), biotite oxidation (Fe(II)), and apatite dissolution (P) (Buss and others, 2008, 2010).

Within the bulk of the rindlet zone, hornblende is relatively stable, whereas plagioclase dissolves at a rate of 90×10^{-14} moles per square meter per second (mol m^{-2} s^{-1}), biotite is oxidized at a rate of 3.1×10^{-14} mol m^{-2} s^{-1}, and apatite dissolves at a rate of 6.8×10^{-14} mol m^{-2} s^{-1} (Buss and others, 2008, 2010). Concurrent with these mineral weathering reactions, the rindlets are further fractured by microcracks. Additional pore space develops by the dissolution of plagioclase; some of the dissolved constituents precipitate within the pore space as kaolinite and gibbsite (Murphy and others, 1998; Turner and others, 2003; Buss and others, 2004, 2008), whereas other constituents, notably Na and Ca, are lost from the profile. Sodium and calcium are abundant in all stream waters within the Icacos Basin (Bhatt and McDowell, 2007), reflecting plagioclase dissolution. The precipitation of kaolinite following plagioclase dissolution leads to an isotopically heavy $\delta^{30}Si$ signature (+0.8 per mil; ratio of stable isotopes of silicon, $^{30}Si/^{28}Si$, relative to international standard NBS-28) in pore waters from the deepest saprolite, because isotopically light Si is preferentially sequestered in the kaolinite (Ziegler and others, 2005). Similarly, Ge/Si ratios in deep saprolite pore waters are low (≈1.0–2.0 micromoles per mole (µmol mol^{-1})) reflecting the dissolution of plagioclase (Ge/Si = 1.5µmol mol^{-1}) and the formation of kaolinite enriched in Ge (Ge/Si = 4.8–6.1 µmol mol^{-1}, Lugolobi and others, 2010). Because plagioclase weathers only in the rindlet zone (White and others, 1998; Turner and others, 2003) and at the rindlet-saprolite interface (Buss and others, 2008), weathering at this interface is the primary control on Si flux into the deep saprolite pore waters. The low Ge/Si ratios of the deep saprolite pore waters are also reflected in stream waters in the Icacos and Guabá watersheds during base flow (Ge/Si ≈ 0.29 µmol mol^{-1}), indicating that weathering at the rindlet zone is the primary contributor to stream-water Si during base flow (Lugolobi and others, 2010; Kurtz and others, 2011). Likewise, the isotopic composition of Si in stream waters in the Icacos watershed ($\delta^{30}Si$ = +1.2 to +1.5 per mil during base flow) reflects weathering reactions (plagioclase and hornblende dissolution) that occur at the bedrock-saprolite interface (Ziegler and others, 2005). During storm events, however, stream-water Ge/Si ratios are higher (2.3 µmol mol^{-1}) and $\delta^{30}Si$ values lower (+0.8 per mil), consistent with the shallow saprolite and soil zone Ge/Si ratios (2.3 to 3.3 and 4.6 µmol mol^{-1}, respectively) and $\delta^{30}Si$ values (–0.8 and –1.4 to –1.7 per mil, respectively), indicating rapid flow of storm waters overland and through shallow subsurface zones (Ziegler and others, 2005; Kurtz and others, 2011).

The removal of soil and saprolite from bedrock and corestone-rindlet assemblages by landslides enhances access of reactants (such as oxygen, carbonic acid, and organic acids) to primary minerals such as plagioclase, hornblende, biotite, and apatite (Frizano and others, 2002; Bhatt and McDowell, 2007). This effect is more pronounced at higher elevations and is revealed in stream waters draining higher elevations (Bhatt and McDowell, 2007). Enhanced access to mineral nutrients contained in primary minerals also aids in the rapid restoration of vegetation on landslide scarps in the Icacos watershed (Frizano and others, 2002).

At the rindlet-saprolite interface, the rindlets finally disaggregate and transform into saprolite (figs. 3, 4). The narrow zone (≈7 cm at the rindlet sequence studied) surrounding the visible interface has been called the protosaprolite zone (Buss and others, 2008) or saprock zone (Minyard and others, 2011). Within this zone, plagioclase and apatite completely dissolve and biotite achieves the oxidized composition found within the saprolite. Also within this zone, hornblende begins to weather and rapidly dissolves to completion at a rate of 1.4×10^{-12} mol m^{-2} s^{-1}, calculated from the solid-state gradient in Fe(II) within the protosaprolite zone (Buss and others, 2008). Thus hornblende provides the dominant flux of Fe(II) to the saprolite and the deep saprolite biota (Buss and others, 2005).

In the deep saprolite, microbial communities are relatively isolated from the biogeochemical cycling near the surface. Nutrients, such as organic carbon and phosphorous, do not infiltrate to the deep saprolite (Murphy, 1995; Buss and others, 2005, 2010). Therefore, the deep communities depend directly upon nutrients and energy sources derived from the rock-forming minerals during weathering of the rindlets and corestones. Apatite dissolution across the rindlet zone and at the rindlet-saprolite interface produces sufficient flux of phosphorous to support the needs of the deep microbial community (Buss and others, 2010). This community includes autotrophic microorganisms that fix CO_2 to produce organic carbon from inorganic carbon. At least some of these autotrophs are also iron oxidizers, which derive energy by oxidizing the Fe(II) that is rapidly released at the rindlet-saprolite interface during hornblende dissolution (Buss and others, 2005, 2008). Iron-oxidizing bacteria contribute to the formation of secondary Fe(III)-oxide minerals (goethite) in the saprolite and potentially affect the rate of spheroidal weathering by decreasing the concentration of dissolved oxygen in pore water (Buss and others, 2005, 2008).

Weathering Processes in the Saprolite and Soil

Saprolite is, by definition, an isovolumetric weathering product (Bates and Jackson, 1984), and this characteristic has been confirmed for the Icacos saprolite by calculations of volumetric strain with respect to Ti (White and others, 1998; Buss and others, 2008) that are close to zero. The 50 percent porosity and visible primary granitic texture of the saprolite is also consistent with isovolumetric weathering (White and others, 1998).

Weathering reactions within the saprolite include the replacement of biotite by kaolinite, quartz dissolution, oxidation of Fe(II) and Mn(II), and precipitation of Fe and Mn oxides (Murphy and others, 1998; White and others, 1998; Buss and others, 2005). These reactions are revealed in gradients in pore-water and solid-state chemistry, in petrographic and electron microscopy of thin sections, and in microbiological assays. Concentrations of K, Mg, and Si in Icacos saprolite pore waters increase with depth, defining weathering gradients (White and others, 1998). Weathering rates for biotite alteration to kaolinite (10^{-15} mol m^{-2} s^{-1}) and for quartz dissolution ($10^{-14.8}$ mol m^{-2} s^{-1}) were calculated from these gradients (Murphy and others, 1998; Schulz and White, 1999).

In the Icacos weathering profile, biotite weathers in two stages. As mentioned earlier, biotite in the corestones and rindlets oxidizes to form an "altered biotite" phase, which is characterized by a d(001) spacing of ≈10.5 Å, and higher Al/Si ratios and lower Fe, Mg, and K contents than fresh biotite (Dong and others, 1998; Murphy and others, 1998; Buss and others, 2008). In the saprolite, altered biotite weathers further to form kaolinite by either of two mechanisms: direct epitaxial overgrowth of two layers of kaolinite onto one layer of altered biotite, or formation of one layer of kaolinite per layer of altered biotite after the formation of an intermediate halloysite layer (Dong and others, 1998; Murphy and others, 1998). The weathering of biotite to kaolinite controls Mg and Si concentrations in pore waters in all but the shallowest and deepest saprolite.

Quartz dissolution in the soil is reflected in Si concentrations (Schulz and White, 1999) and Si isotope ratios (Ziegler and others, 2005) in the pore waters. Quartz dissolution rates under natural conditions are extremely slow, and thus residual quartz is the major structural component of many weathering profiles, including the Icacos saprolite, where quartz abundances and grain size distributions are approximately constant with depth. However, these quartz grains are not inert but show evidence of dissolution in the form of etch pits (Schulz and White, 1999). Quartz dissolution rates, calculated from silica concentrations in the pore waters, are fastest at shallow depths (2.8×10^{-15} mol m^{-2} s^{-1} at 1.5 m depth), where quartz-grain etch pits are the most abundant (Schulz and White, 1999). Silica concentrations in the saprolite pore waters increase linearly with depth, whereas quartz weathering rates decrease with depth. Quartz dissolution also controls the $\delta^{30}Si$ signature in the soil pore waters (–1.4 to –1.7 per mil, Ziegler and others, 2005). Some kaolinite in the shallow soil dissolves in association with lower pH and elevated concentrations of Al and dissolved organic carbon in the soil pore waters (White and others, 1998). Dissolution by organic acids and other organic ligands produced by soil microorganisms and vegetation are likely responsible for the loss of kaolinite in the soil layer, as has been observed in laboratory studies (for example, Maurice and others, 2001) and in other tropical soils (for example, Chorover and Sposito, 1995). However, despite the influence of quartz and kaolinite dissolution, pore-water chemistry in the soil and shallow saprolite is dominated by atmospheric deposition and biological cycling (White and others, 1998; Pett-Ridge and others, 2009; Lugolobi and others, 2010) rather than mineral weathering processes.

Summary

Calculated bedrock weathering rates for the Icacos and Mameyes watersheds are high compared with watersheds around the world that are underlain by siliceous bedrock. Rapid weathering produces thick, highly leached saprolites in both watersheds that decouple subsurface processes from those in the soil. The quartz diorite bedrock in the Icacos watershed weathers spheroidally, forming relatively unweathered bedrock corestones that are surrounded by concentric layers of rock called rindlets. The spheroidal weathering process produces two controlling weathering interfaces. First, disaggregation of the intact rock is initiated at the bedrock-rindlet interface, where biotite oxidation within the corestones leads to spheroidal fracturing. The second controlling interface is the rindlet-saprolite boundary, where the rindlets disintegrate into saprolite owing to the development of extensive pore space and the complete dissolution of plagioclase and hornblende. Stream-water chemistry at base flow within the Río Icacos and its tributaries reflects these rindlet-zone weathering processes. Within the saprolite, biotite is replaced by kaolinite and quartz dissolves. The geochemistry of the overlying soil layer is dominated by the biological recycling of mineral nutrients, but it is also influenced by the dissolution of quartz and kaolinite. These shallow weathering processes are reflected in stream-water chemistry during storm events.

References

Bates, R.L., and Jackson, J.A., 1984, Dictionary of geological terms: Falls Church, Va., The American Geological Institute, 571 p.

Bawiec, W. J., 1998, Geology, geochemistry, geophysics, mineral occurrences, and mineral resource assessment for the commonwealth of Puerto Rico: U.S. Geological Survey Open-File Report 98–38, CD-ROM.

Begle, E.A., 1978, The weathering of granite, Llano region, central Texas: Austin, The University of Texas at Austin, 163 p.

Bhatt, M.P., and McDowell, W.H., 2007, Controls on major solutes within the drainage network of a rapidly weathering tropical watershed: Water Resources Research, v. 43, n. W11402, p. 1–9.

Bisdom, E.B.A., 1967, The role of micro-crack systems in the spheroidal weathering of an intrusive granite in Galicia (NW Spain): Geologie en Mijnbouw, v. 46, p. 333–340.

Briggs, R.P., and Aguilar-Cortés, E., 1980, Geologic map of the Fajardo and Cayo Icacos quadrangles, Puerto Rico: U.S. Geological Survey Miscellaneous Geologic Investigations Map I–1153, scale 1:20000, 1 sheet.

Brown, E.T., Stallard, R., Larsen, M.C., Raisbeck, G.M., and Yiou, F., 1995, Denudation rates determined from the accumulation of in situ–produced ^{10}Be in the Luquillo Experimental Forest, Puerto Rico: Earth and Planetary Science Letters, v. 129, p. 193–202.

Buss, H.L., Bruns, M.A., Schultz, M.J., Moore, J., Mathur, C.F., and Brantley, S.L., 2005, The coupling of biological iron cycling and mineral weathering during saprolite formation, Luquillo Mountains, Puerto Rico: Geobiology, v. 3, p. 247–260.

Buss, H.L., Mathur, R., White, A.F., and Brantley, S.L., 2010, Phosphorus and iron cycling in deep saprolite, Luquillo Mountains, Puerto Rico: Chemical Geology, v. 269, p. 52–61.

Buss, H.L., Sak, P.B., Webb, S.M., and Brantley, S.L., 2008, Weathering of the Rio Blanco quartz diorite, Luquillo Mountains, Puerto Rico—Coupling oxidation, dissolution, and fracturing: Geochimica et Cosmochimica Acta, v. 72, p. 4488–4507.

Buss, H.L., Sak, P.B., White, A.F., and Brantley, S.L., 2004. Mineral dissolution at the granite-saprolite interface, *in* Wanty, R.B., and Seal, R.R.I., eds., International Symposium on Water-Rock Interaction, 11th: Saratoga Springs, N.Y., 27 June–2 July 2004, Taylor and Francis, p. 819–823.

Chatterjee, A., and Raymahashay, B.C., 1998, Spheroidal weathering of Deccan Basalt—A three-mineral model: Quarterly Journal of Engineering Geology, v. 31, p. 175–179.

Chorover, Jon, and Sposito, G., 1995, Surface charge characteristics of kaolinitic tropical soils: Geochimica et Cosmochimica Acta, v. 59, p. 875–884.

Dong, Hailiang, Peacor, D.R., and Murphy, S.F., 1998, TEM study of progressive alteration of igneous biotite to kaolinite throughout a weathered soil profile: Geochimica et Cosmochimica Acta, v. 62, p. 1881–1887.

Dosseto, Anthony, Buss, H., and Suresh, P.O., 2011, The delicate balance between soil production and erosion, and its role on landscape evolution: Applied Geochemistry, v. 26, S24-S27.

Eberl, D.D., 2003, User guide to RockJock—A program for determining quantitative mineralogy from X-ray diffraction data: U.S. Geological Survey Open-File Report 03–78, 36 p.

Eggler, D.H., Larson, E.E., and Bradley, W.C., 1969, Granites, grusses, and the Sherman erosion surface, southern Laramie Range, Colorado-Wyoming: American Journal of Science, v. 267, p. 510–522.

Farmin, Rollin, 1937, Hypogene exfoliation in rock masses: Journal of Geology, v. 45, p. 625–635.

Fletcher, R.C., Buss, H.L., and Brantley, S.L., 2006, A spheroidal weathering model coupling porewater chemistry to soil thicknesses during steady-state denudation: Earth and Planetary Science Letters, v. 244, p. 444–457.

Freyssinet, Phillipe, and Farah, A.S., 2000, Geochemical mass balance and weathering rates of ultramafic schists in Amazonia: Chemical Geology, v. 170, p. 133–151.

Fritz, S.J., and Ragland, P.C., 1980, Weathering rinds developed on plutonic igneous rocks in the North Carolina piedmont: American Journal of Science, v. 280, p. 546–559.

Frizano, Jacqueline, Johnson, A.H., and Vann, D.R., 2002, Soil phosphorus fractionation during forest development on landslide scars in the Luquillo Mountains, Puerto Rico: Biotropica, v. 34, p. 17–26.

Isherwood, Dana, and Street, A., 1976, Biotite-induced grussification of the Boulder Creek Granodiorite, Boulder County, Colorado: Geological Society of America Bulletin, v. 87, p. 366–370

Jolly, W.T., Lidiak, E.G., Schellekens, J.H., and Santos, J., 1998, Volcanism, tectonic and stratigraphic correlations in Puerto Rico, *in* Lidiak, E.G., and Larue, D.K., eds., Tectonics and geochemistry of the northeastern Caribbean: Geological Society of America Special Paper 322, p. 1–34.

Kurtz, A.C., Lugolobi, F., and Salvucci, G., 2011, Germanium-silicon as a flowpath tracer—Application to the Río Icacos watershed: Water Resources Research, v. 47, W06516.

Larsen, E.S., 1948, Batholith and associated rocks of Corona, Elsinore and San Luis Rey quadrangles, southern California: Geological Society of America Memoir, v. 29, p. 114–119.

Larsen, M.C., and Torres-Sánchez, A.J., 1998, The frequency and distribution of recent landslides in three montane tropical regions of Puerto Rico: Geomorphology, v. 24, p. 309–331.

Lugolobi, Festo, Kurtz, A.C., and Derry, L.A., 2010, Germanium-silicon fractionation in a tropical, granitic weathering environment: Geochimica et Cosmochimica Acta, v. 74, p. 1294–1308.

Maurice, P.A., Vierkorn, M.A., Hersman, L.E., and Fulghum, J.E., 2001, Dissolution of well and poorly ordered kaolinites by an aerobic bacterium: Chemical Geology, v. 180, p. 81–97.

Meybeck, Michel, 1987, Global chemical weathering of surficial rocks estimated from dissolved river loads: American Journal of Science, v. 287, p. 401–428.

Minyard, M.L., Bruns, M.A., Martinez, C.E., Liermann, L.J., Buss, H.L., and Brantley, S.L., 2011, Halloysite nanotubes and bacteria at the saprolite-bedrock interface, Rio Icacos watershed, Puerto Rico: Soil Science Society of America Journal, v. 75, p. 348–356.

Murphy, S.F., 1995, The weathering of biotite in a tropical forest soil, Luquillo Mountains, Puerto Rico: State College, Pennsylvania State University Master's thesis, 100 p.

Murphy, S.F., Brantley, S.L., Blum, A.E., White, A.F., and Dong, H., 1998, Chemical weathering in a tropical watershed, Luquillo Mountains, Puerto Rico—II. Rate and mechanism of biotite weathering: Geochimica et Cosmochimica Acta, v. 62, p. 227–243.

Murphy, S.F., Stallard, R.F., Larsen, M.C., and Gould, W.A., 2012, Physiography, geology, and land cover of four watersheds in eastern Puerto Rico, ch. A *in* Murphy, S.F., and Stallard, R.F., eds., Water quality and landscape processes of eastern Puerto Rico: U.S. Geological Survey Professional Paper 1789, p. 1–24.

Navarre-Sitchler, Alexis, and Brantley, S., 2007, Basalt weathering across scales: Earth and Planetary Science Letters, v. 261, p. 321–334.

Ollier, C.D., 1971, Causes of spheroidal weathering: Earth-Science Reviews, v. 7, p.127–141.

Pett-Ridge, J.C., Derry, L.A., and Kurtz, A.C., 2009, Sr isotopes as a tracer of weathering processes and dust inputs in a tropical granitoid watershed, Luquillo Mountains, Puerto Rico: Geochimica et Cosmochimica Acta, v. 73, p. 25–43.

Riebe, C.S., Kirchner, J.W., and Finkel, R.C., 2003, Long-term rates of chemical weathering and physical erosion from cosmogenic nuclides and geochemical mass balance: Geochimica et Cosmochimica Acta, v. 67, p. 4411–4427.

Riebe, C.S., Kirchner, J.W., and Finkel, R.C., 2004, Erosional and climatic effects on long-term chemical weathering rates in granitic landscapes spanning diverse climate regimes: Earth and Planetary Science Letters, v. 224, p. 547–562.

Schellekens, Jaap, Scatena, F.N., Bruijnzeel, L.A., van Dijk, A.I.J.M., Groen, M.M.A., and van Hogezand, R.J.P., 2004, Stormflow generation in a small rainforest catchment in the Luquillo Experimental Forest, Puerto Rico: Hydrological Processes, v. 18, p. 505–530.

Schulz, M.S., and White, A.F., 1999, Chemical weathering in a tropical watershed, Luquillo Mountains, Puerto Rico—III. Quartz dissolution rates: Geochimica et Cosmochimica Acta, v. 63, p. 337–350.

Seiders, V.M., 1971, Geologic map of the El Yunque quadrangle, Puerto Rico. U.S. Geological Survey Miscellaneous Geological Investigation I–658, 1 sheet, scale 1:20,000; available at *http://pubs.er.usgs.gov/publication/i658*

Simpson, D.R., 1964, Exfoliation of the Upper Pocohontas sandstone, Mercer County, West Virginia: American Journal of Science, v. 242, p. 545–551.

Smith, A.L., Schellekens, J.H., and Diaz, A.M., 1998, Batholiths as markers of tectonic change in the northeastern Caribbean: Geological Society of America Special Paper, v. 322, p. 99–122.

Stallard, R.F., and Edmond, J.M., 1983, Geochemistry of the Amazon—2. The influence of geology and weathering environment on the dissolved load: Journal of Geophysical Research, v. 88, p. 9671–9688.

Turner, B.F., Stallard, R.F., and Brantley, S.L., 2003, Investigation of in situ weathering of quartz diorite bedrock in the Río Icacos Basin, Luquillo Experimental Forest, Puerto Rico: Chemical Geology, v. 202, p. 313–341.

White, A.F., 2002, Determining mineral weathering rates based on solid and solute weathering gradients and velocities—Application to biotite weathering in saprolites: Chemical Geology, v. 190, p. 69–89.

White, A.F., Blum, A.E., Schulz, M.S., Vivit, D.V., Stonestrom, D.A., Larsen, M., Murphy, S.F., and Eberl, D., 1998, Chemical weathering in a tropical watershed, Luquillo Mountains, Puerto Rico—I. Long-term versus short-term weathering fluxes: Geochimica et Cosmochimica Acta, v. 62, p. 209–226.

Ziegler, Karen, Chadwick, O.A., White, A., and Brzezinski, M.A., 2005, δ^{30}Si systematics in a granitic saprolite, Puerto Rico: Geology, v. 33, p. 817–820.